

InSb nanostructures: Growth, Morphology control and transport properties

Isha Verma



SCUOLA
NORMALE
SUPERIORE

Supervisor: Prof. Lucia Sorba

**National Enterprise for Nanoscience and Nanotechnology (NEST)
Scuola Normale Superiore (SNS)
Pisa, Italy**

OUTLINE



❖ **Introduction**

❖ **Part 1: InSb morphology control on InAs stem**



❖ **Part 2: InSb nanoflags on InP stem**

❖ **Part 3: Morphological evolution of InSb nanoflags model**

❖ **Part 4: Electronic properties of InSb nanoflags based devices**



❖ **Conclusions**

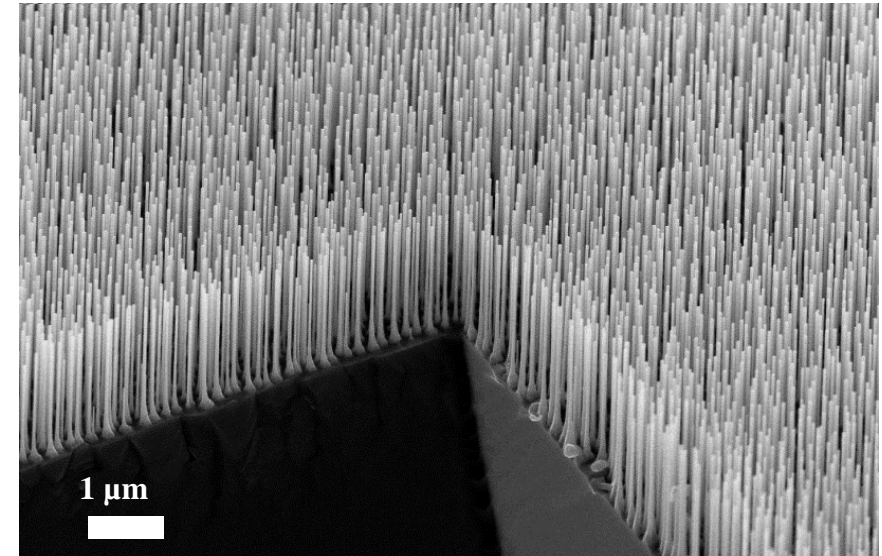
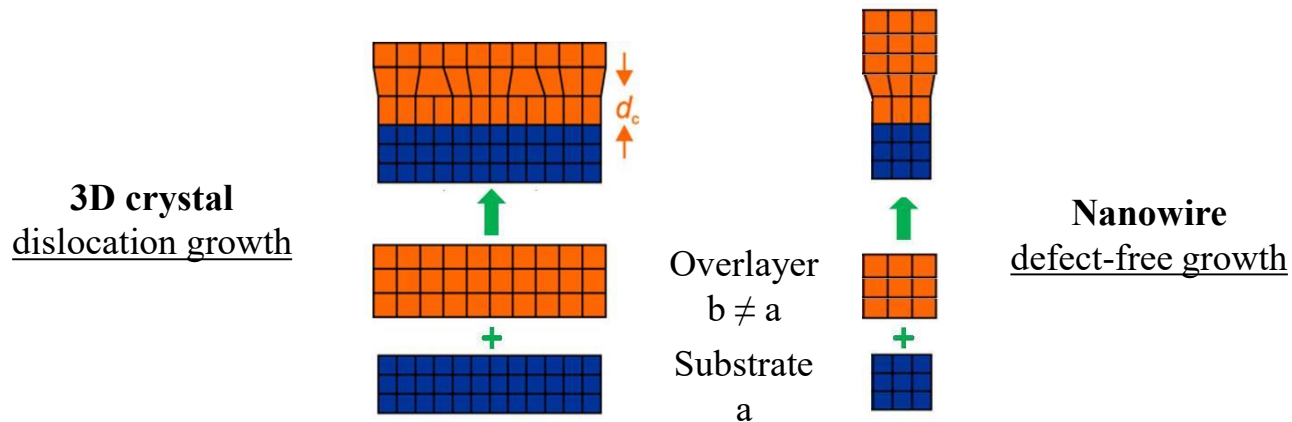
Semiconductor Nanostructures

❑ **Semiconductor NWs** → quasi-one dimensional crystalline structures (diameters typically < 100 nm & length of several μm)

❑ **Novel properties:**

- ✓ Free standing nature
- ✓ High surface/volume ratio
- ✓ Efficient strain relaxations
- ✓ Defect-free growth of heterostructures
- ✓ Carriers confinement

Heteroepitaxy: bulk crystal vs nanowires



❑ **Technological relevance:** applications in electronics, photonics, chemical sensing...

Nanowire growth mechanisms

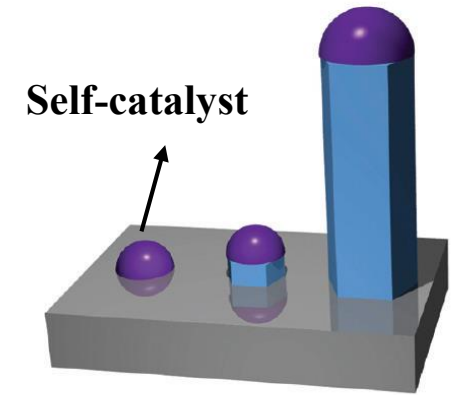
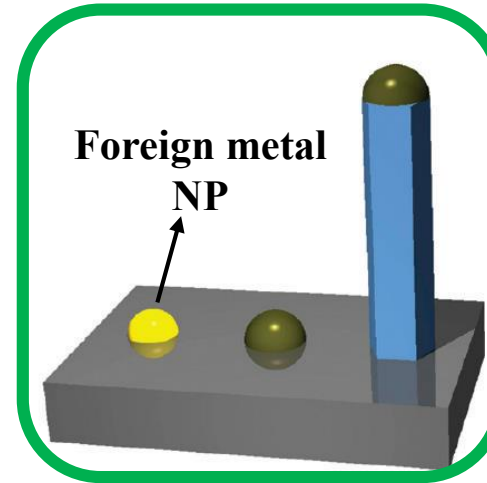
Vapor-Liquid-Solid (VLS)

- Foreign metal assisted
- Self-catalyzed

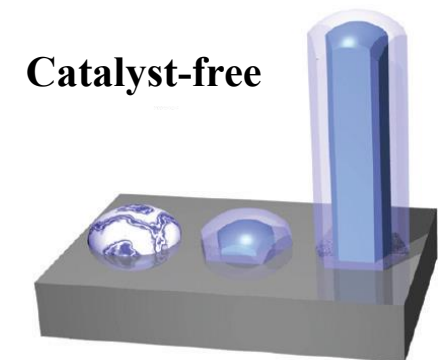
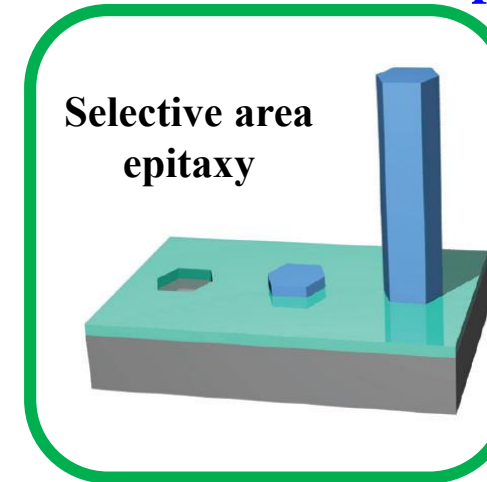
Vapor-Solid (VS)

- Selective area epitaxy (SAE)
- Self-induced or catalyst-free

Vapor-Liquid-Solid (VLS)



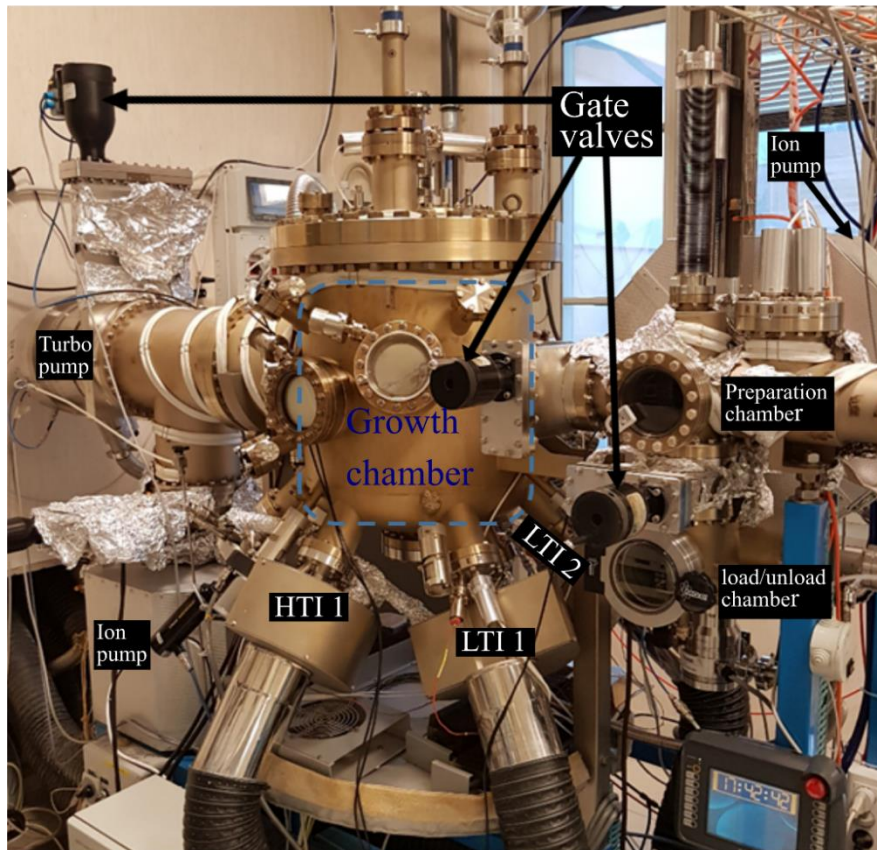
Vapor-Solid (VS)



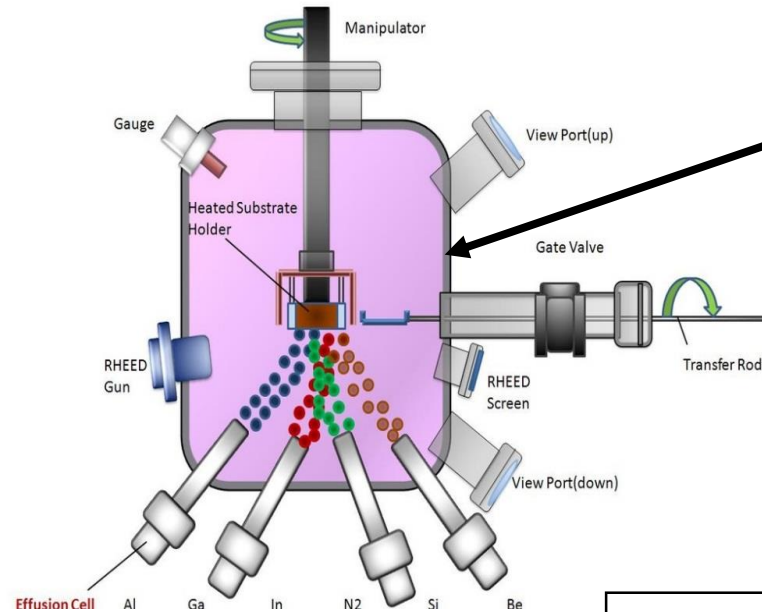
Chemical Beam Epitaxy (CBE)

CBE system at NEST lab

Riber Compact-21 CBE for the growth of III-V NWs



Schematic of CBE



Ultra High Vacuum (UHV) growth chamber
(base pressure: 10^{-9} Torr)

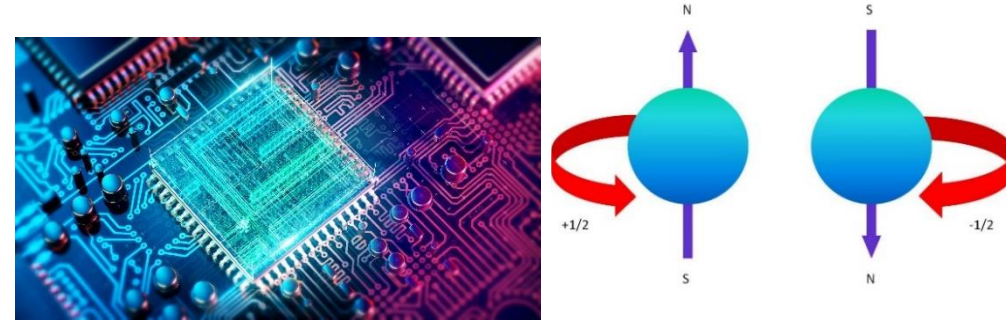
Metal-organic precursors
Group III : TMI_n, TEGa, TMAI
Group V : TBAs, TBP, TDMASb,
TMSb
n-doping : TBSe

Advantages of CBE system
Direct control of fluxes
Monolayer thickness control
Abrupt interfaces
Good control of composition and doping profiles

InSb: Motivation & Challenges

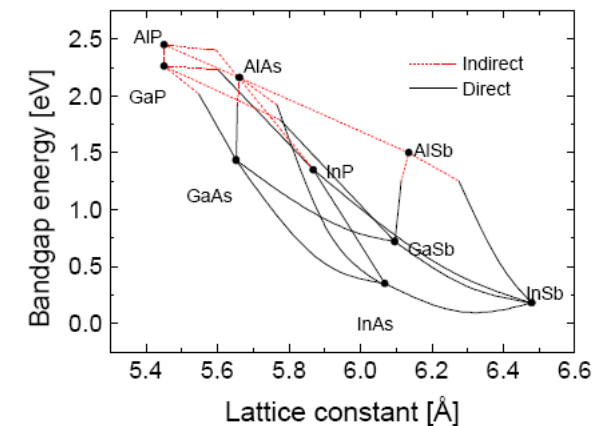
InSb Heterostructures:

- ❑ Narrow bandgap \longrightarrow mid-infrared optoelectronic devices
- ❑ High bulk electron mobilities ($7.7 \times 10^4 \text{ cm}^2/(\text{Vs})$), small effective mass ($0.018 m_e$) \longrightarrow high-speed and low-power electronic devices
- ❑ Strong spin-orbit interaction, large Landé g-factor (~ 50) \longrightarrow spintronics and topological quantum computing



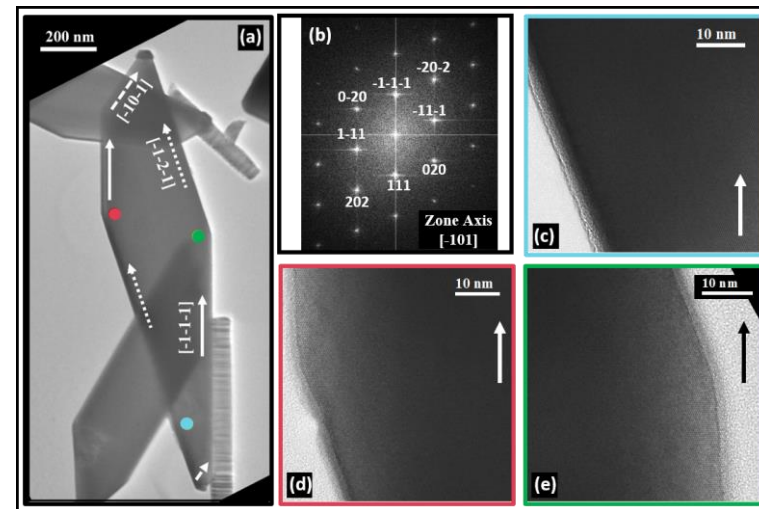
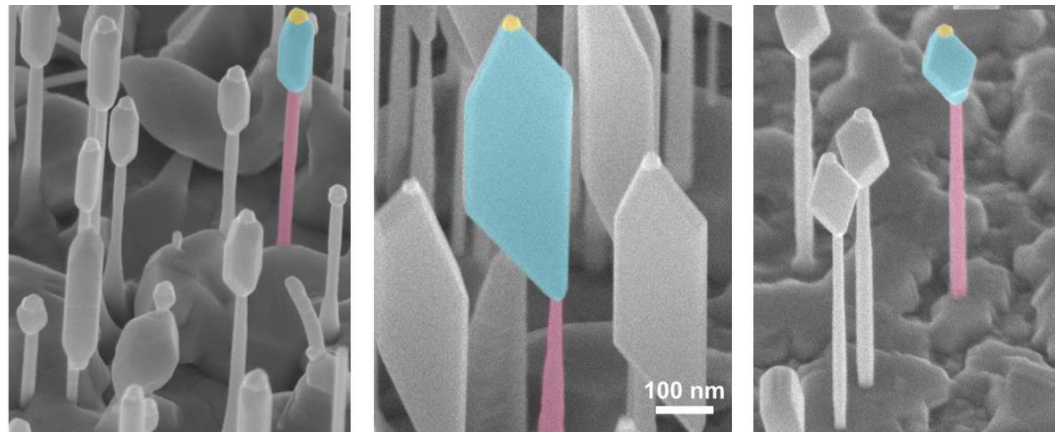
Growth Challenges:

- ❑ 2D Epitaxial growth of InSb \longrightarrow large lattice mismatch with common SC substrates
- ❑ Solution \longrightarrow InSb nanostructure growth on nanowire stem (efficient strain relaxation)
- ❑ Low Sb vapor pressure and surfactant effects \longrightarrow difficult to control the morphology; a detailed explanation of the growth mechanism and morphology tuning is required.



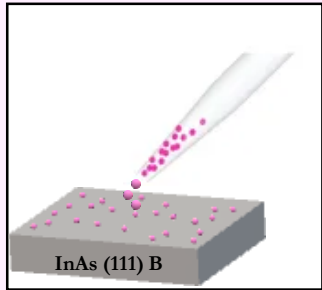
Part 1

InSb morphology control by tuning growth parameters on InAs stem

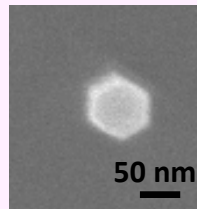
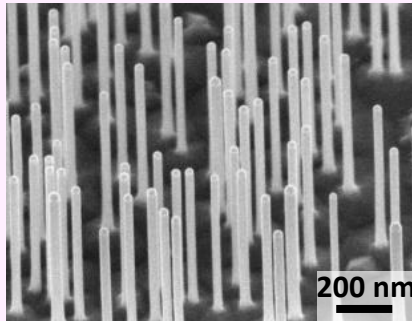
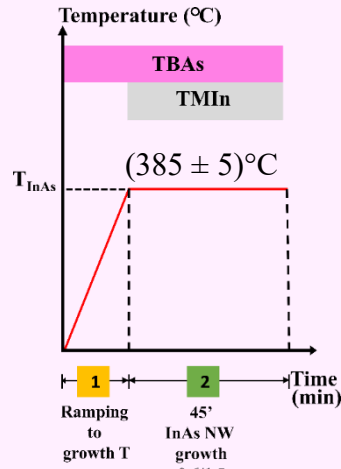


InSb growth temperature

InAs NW stem

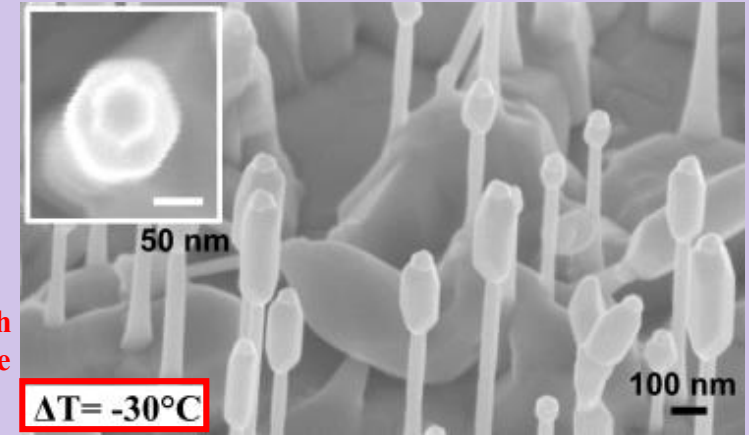
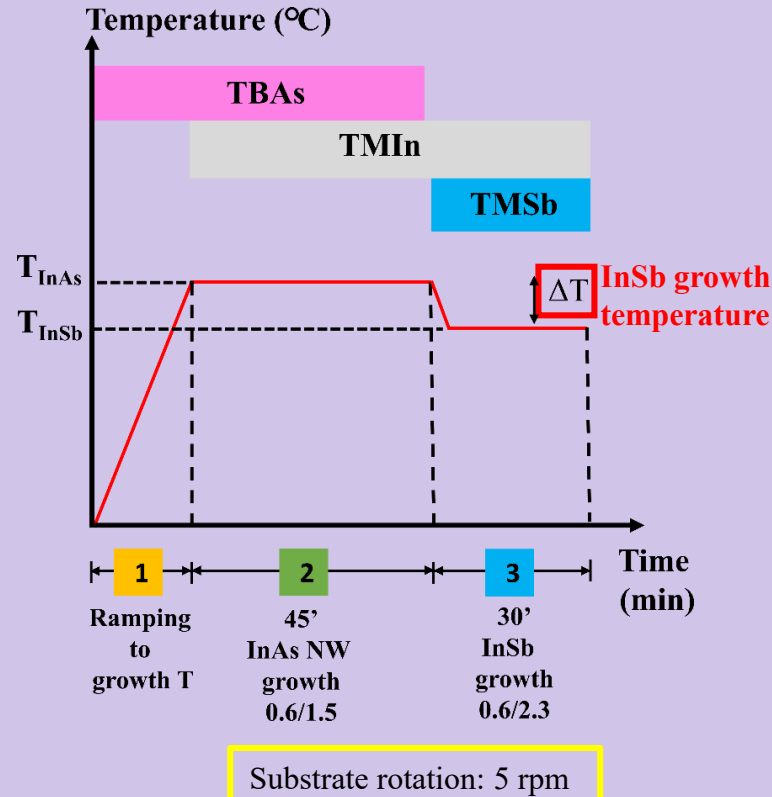


Drop-cast 30 nm Au colloids on InAs 111B

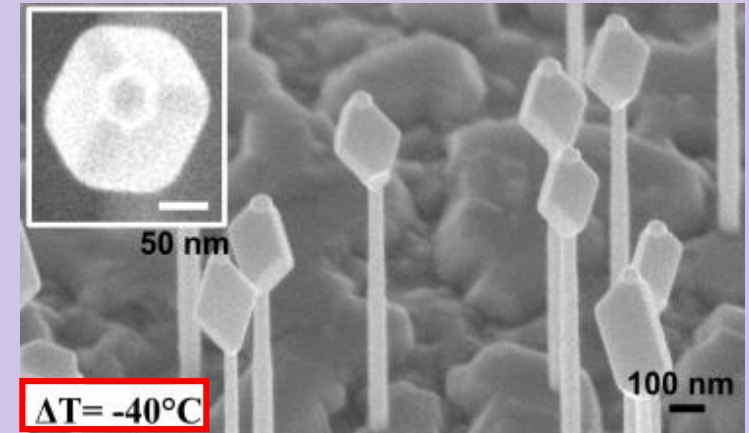


Length=800 ± 26 nm, Diameter= 41 ± 2 nm

InSb growth temperature



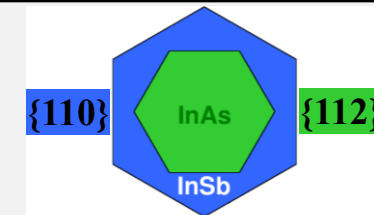
Length=(291 ± 46) nm, diameter=(94 ± 12) nm



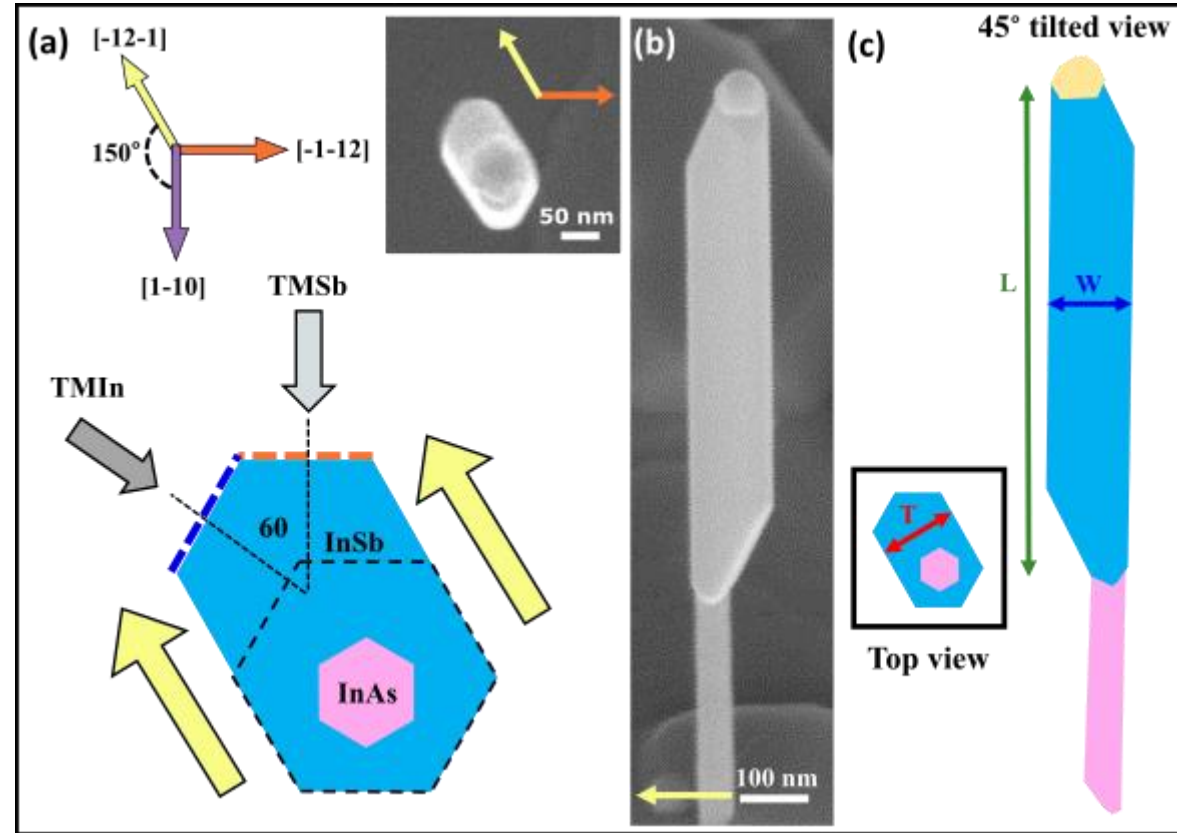
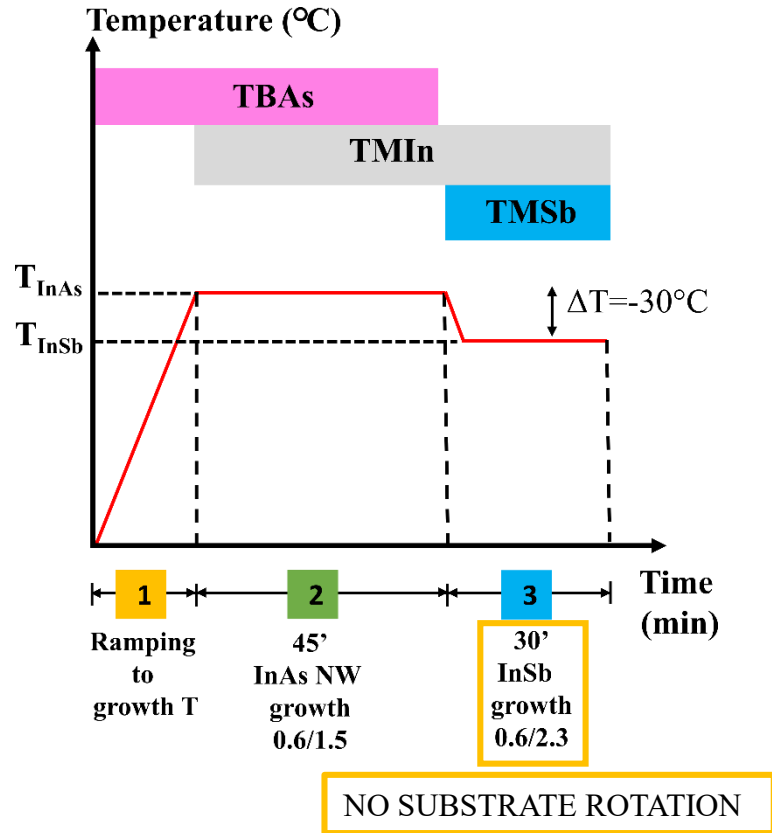
Length=(314 ± 32) nm, diameter=(148 ± 14) nm

Conclusions

- InAs and InSb have 30° rotated side facets.
- InSb radial growth rate is enhanced at lower growth temperatures and hence a 3D morphology is favored.



Substrate rotation & Orientation



$L = (1048 \pm 108) \text{ nm}$, $W = (112 \pm 18) \text{ nm}$, $T = (87 \pm 2) \text{ nm}$

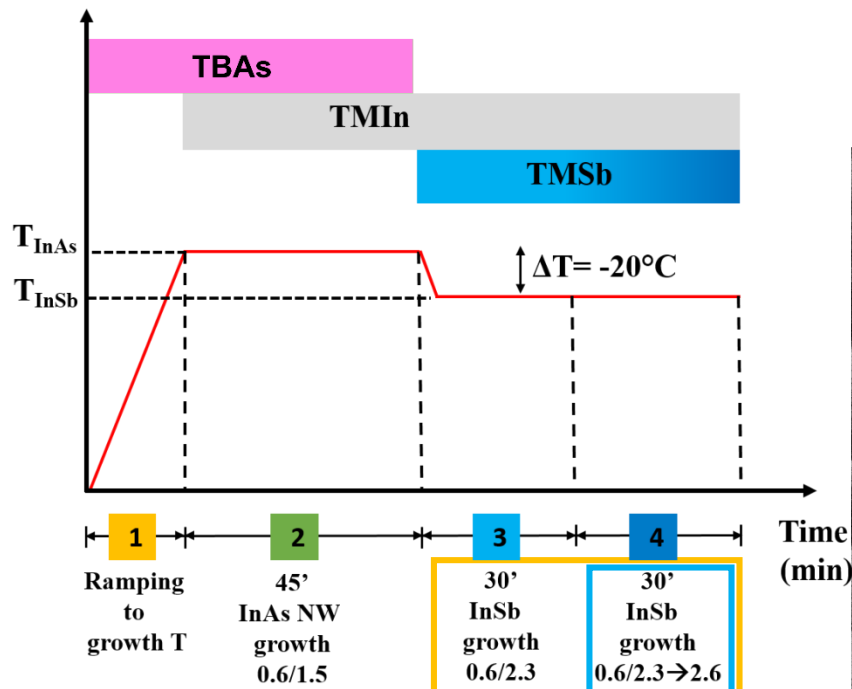
Asymmetric InSb NW growth

- Stopping the substrate rotation before initiating InSb growth triggers asymmetric growth.
- Alining the cleaved edge surface $\{110\}$ of the substrate facing the TMSb injector, so that the projection of the Sb beam impingement direction on the substrate surface is perpendicular to one of the six $\{110\}$ sidewalls of the InSb NW.
- InSb is elongated along $[-12-1]$ direction.

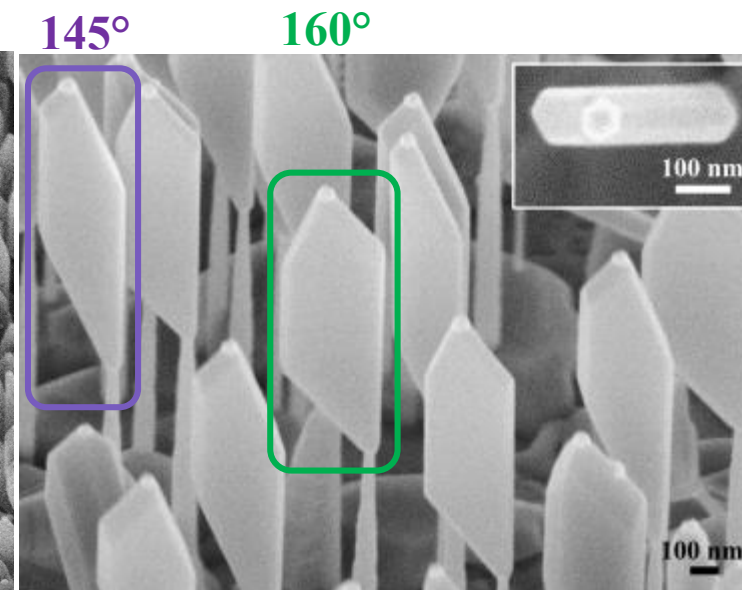
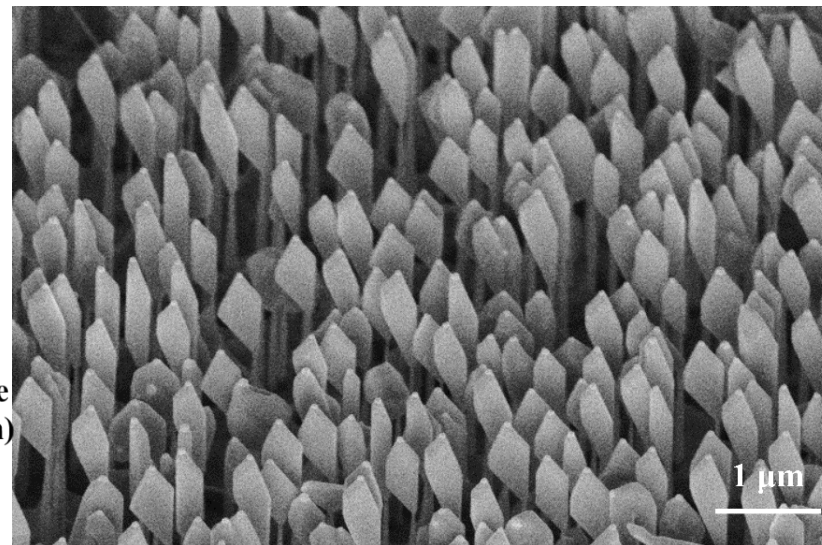
Sb flux gradient

Free-standing InSb Nanoflag

Temperature (°C)



NO SUBSTRATE ROTATION



$L = (1.3 \pm 0.1) \mu m$, $W = (282 \pm 87) nm$, $T = (104 \pm 17) nm$

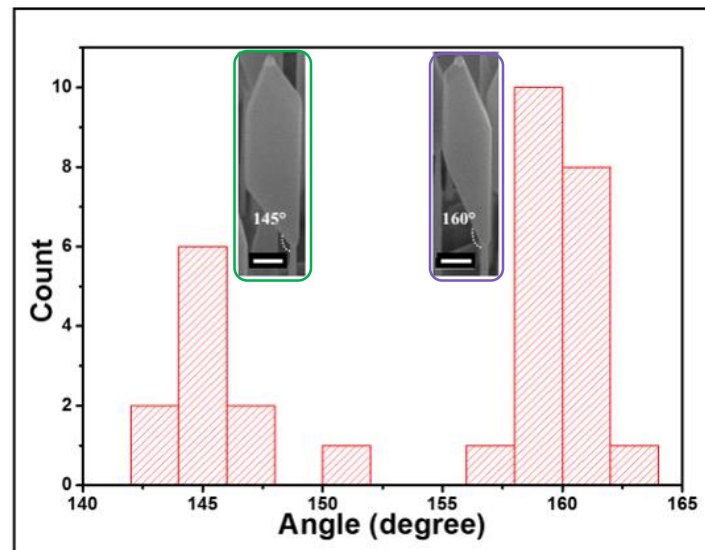
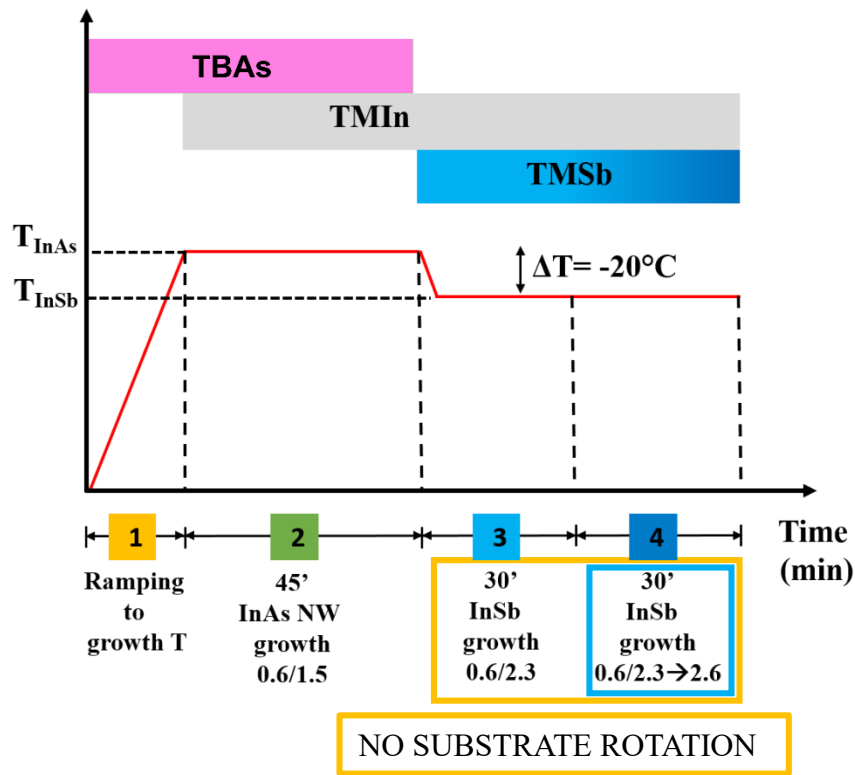
InSb NF growth

- Additional 30' InSb growth with linearly increasing TMSb from 2.3 Torr to 2.6 Torr without substrate rotation → asymmetric growth enhancement.
- Nearly 100% yield of NFs.
- 2 families of NFs with aperture angles of about 145° and 160° elongated in the same direction.

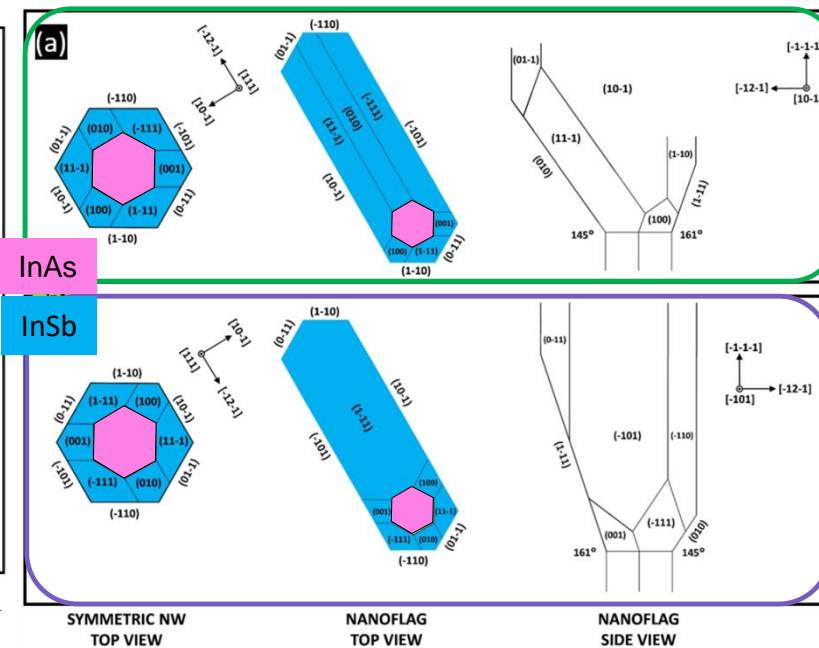
Sb flux gradient

Free-standing InSb Nanoflag

Temperature (°C)



180° rotation around the growth axis of the additional facets at the interface

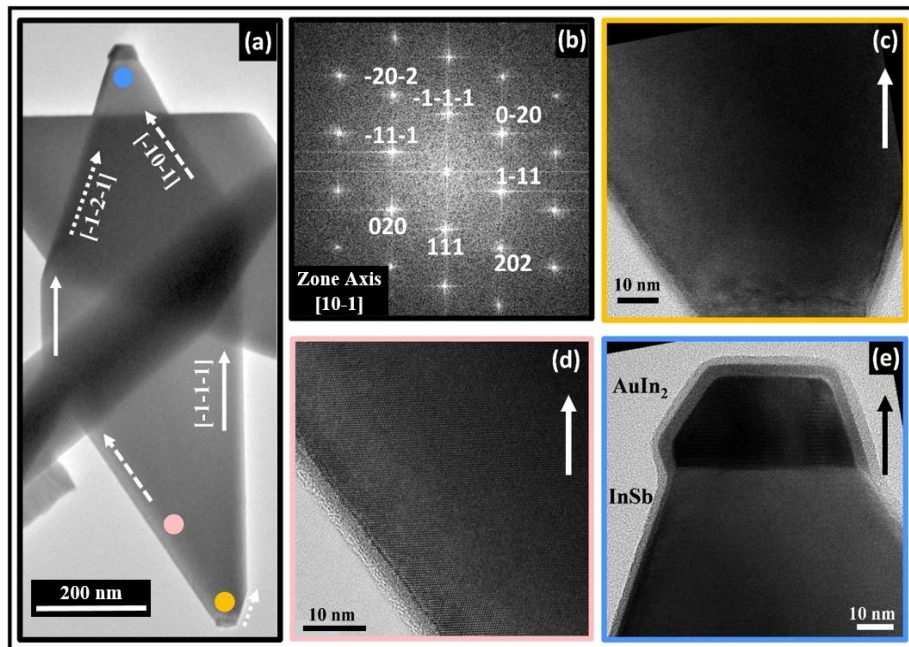


InSb NF growth

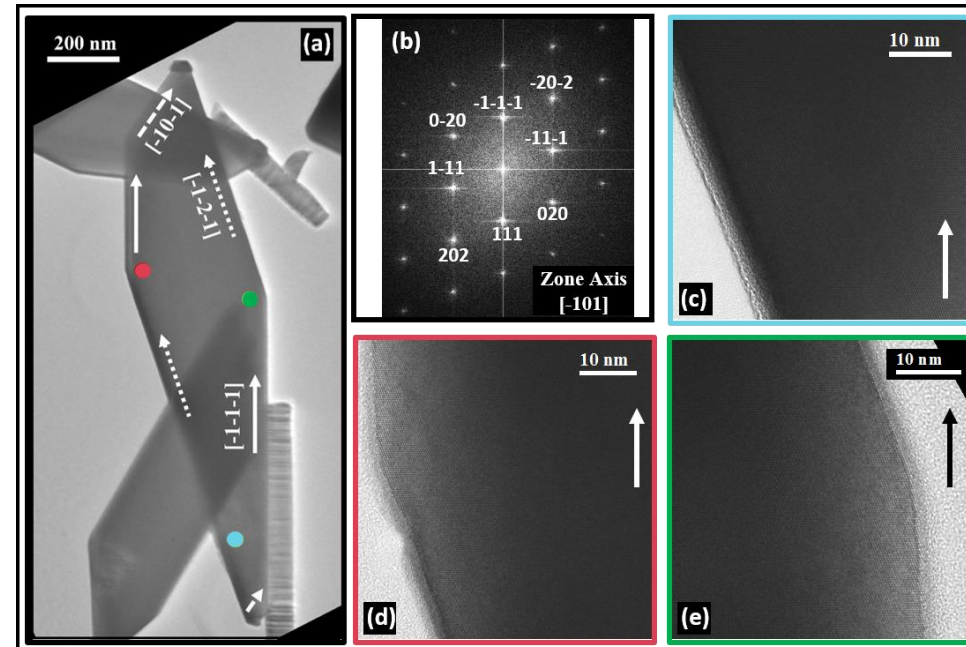
- Additional 30' InSb growth with linearly increasing TMSb from 2.3 Torr to 2.6 Torr without substrate rotation → asymmetric growth enhancement.
- Nearly 100% yield of NFs.
- 2 families of NFs with aperture angles of about 145° and 160° elongated in the same direction.

Transmission electron microscopy

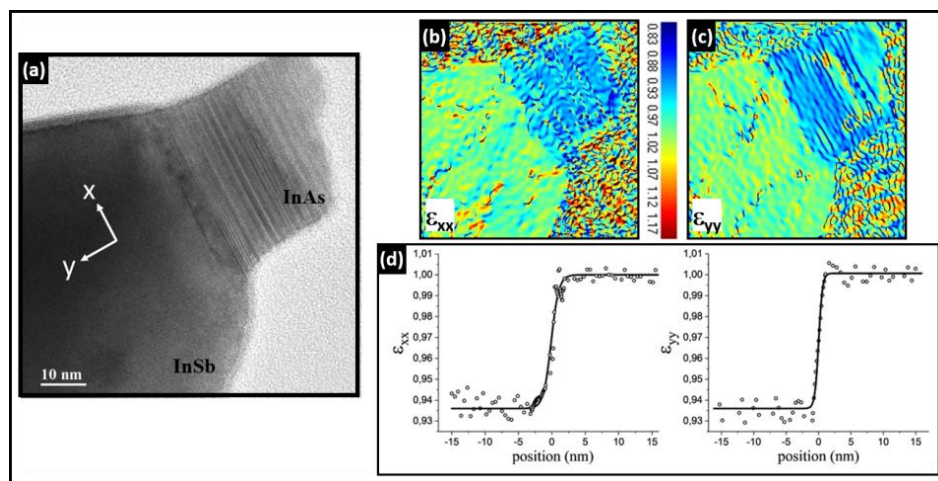
145° aperture angle



160° aperture angle



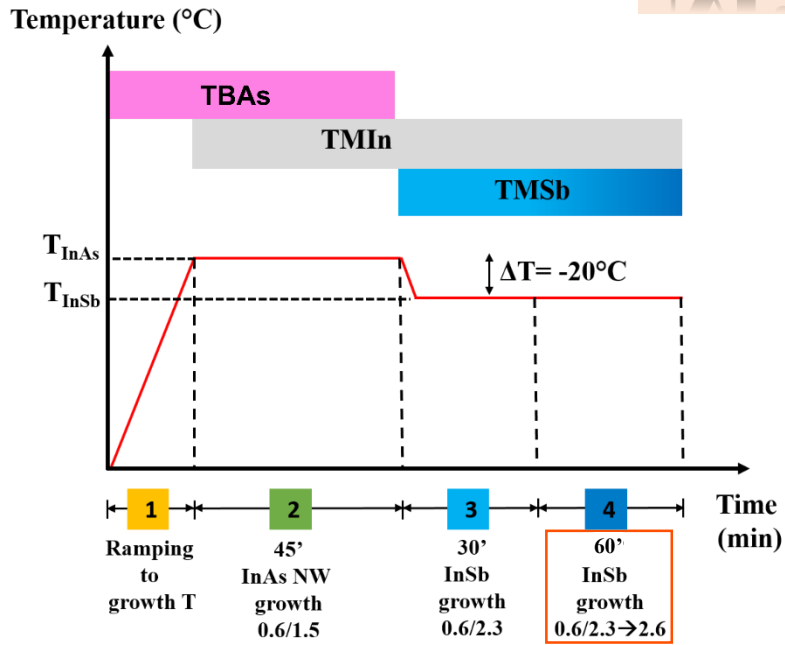
Geometrical phase analysis



Conclusions

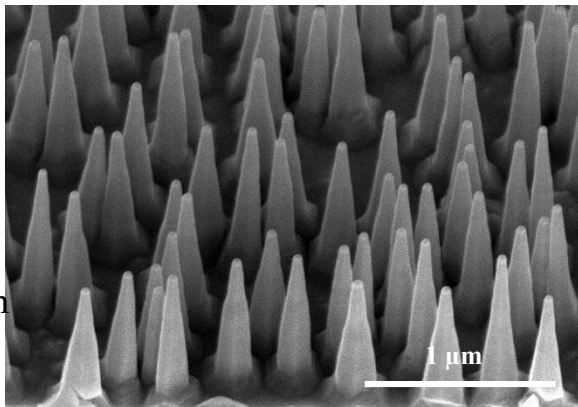
- Defect-free ZB crystal structure.
- Stoichiometric composition.
- Relaxed lattice parameter.

Maximizing 2D InSb



Increasing InSb growth time

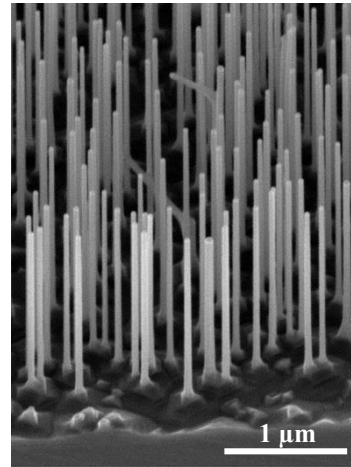
InP NW stem



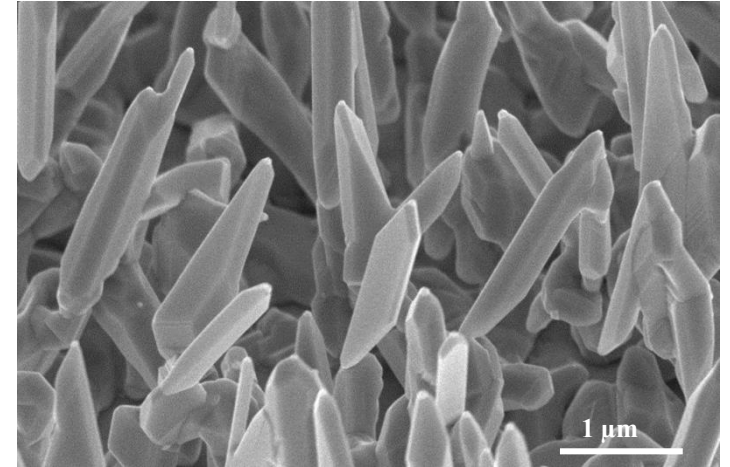
$L = 867 \pm 101$ nm
 Tip $D = 55 \pm 5$ nm
 Base $D = 173 \pm 36$ nm

60' InP (0.6/1.2) @ $T_{InP} = 400^\circ C$ on InP 111B substrate

InAs stem



InSb NFs grown for longer time



Problem

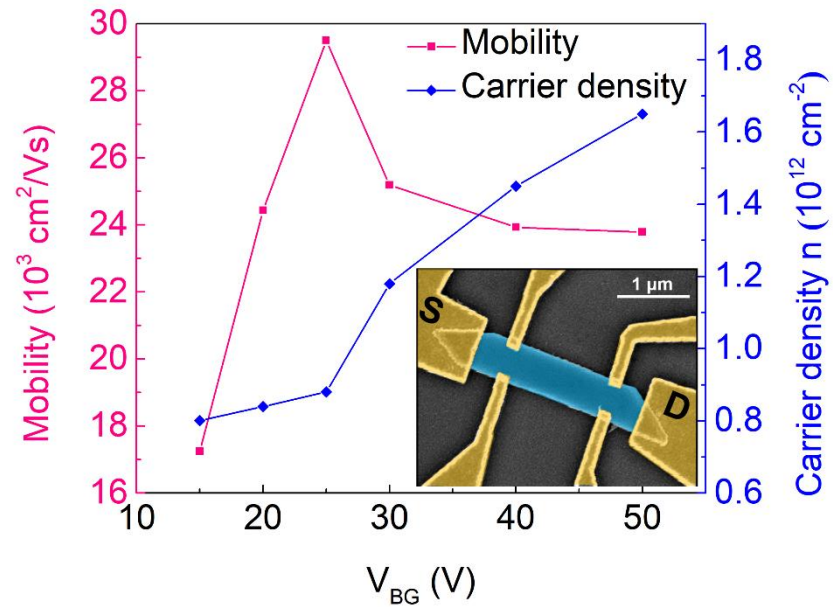
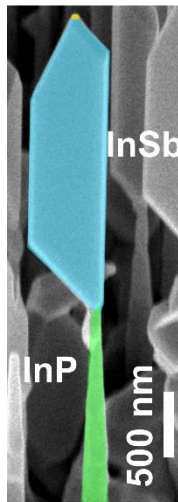
- InSb segments grows larger with increase in growth time.
- Thin untapered InAs stem bends, leading to loss of alignment with the precursor fluxes and consequently of the InSb orientation.
- Preferential growth direction vanishes, and 3D-like InSb structures are obtained.

Solution

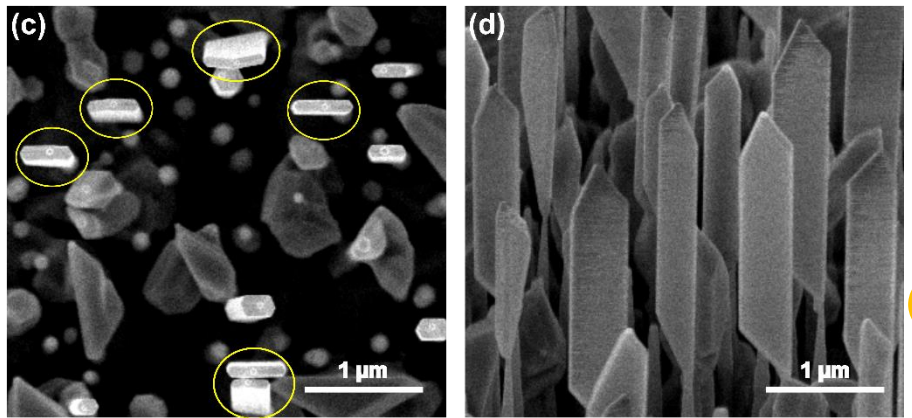
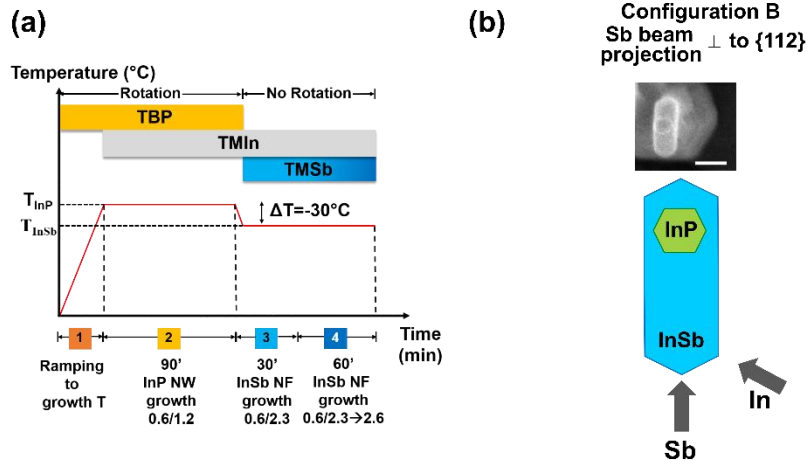
- We need more robust NW stem, like tapered InP NWs, instead of thin untapered InAs stems.

Part 2

InSb nanoflags on InP NW stems



InSb NFs on InP NW stem



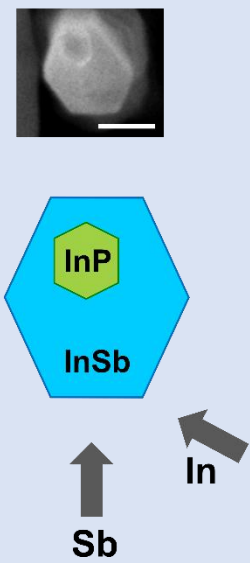
$L = (2.8 \pm 0.2) \mu\text{m}$
 $W = (470 \pm 80) \text{nm}$
 $T = (105 \pm 20) \text{nm}$

$(W/T) \geq 4 \sim 40\%$

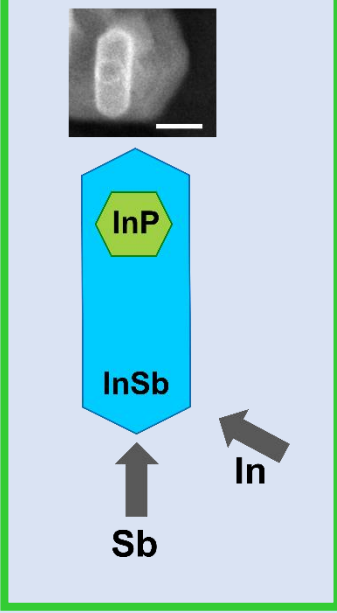
- InP NW stems were grown with sample rotation for 90' to provide more sturdy support, followed by InSb growth at $\Delta T = -30^\circ\text{C}$ without rotation with an abrupt switch in group V flux from TBP to TMSb without variation in the TMIn flux.
- An additional 60' of growth, linearly increasing the TMSb line pressure. Sb flux grading helps to enhance the asymmetric growth, increasing the lateral dimensions of the NFs.
- How to decouple W & T: **growth model**.

Configurations

Configuration A
 Sb beam \perp to {110}



Configuration B
 Sb beam \perp to {112}



- When the sample is oriented in **configuration A**, only the 3 backside InSb facets (opposite to the Sb beam) are totally screened from Sb impingement, while the sidewall perpendicular to the Sb beam projection will receive the direct beam, and the two adjacent inclined facets will be reached by the beam at grazing incidence: NFs will be larger and less elongated.
- In **configuration B**, there are only two {110} facets facing the Sb injector, that is, reached by direct impingement, so the growth rate on these two facets will be higher compared to the other four sidewalls, and we obtain thinner flags.

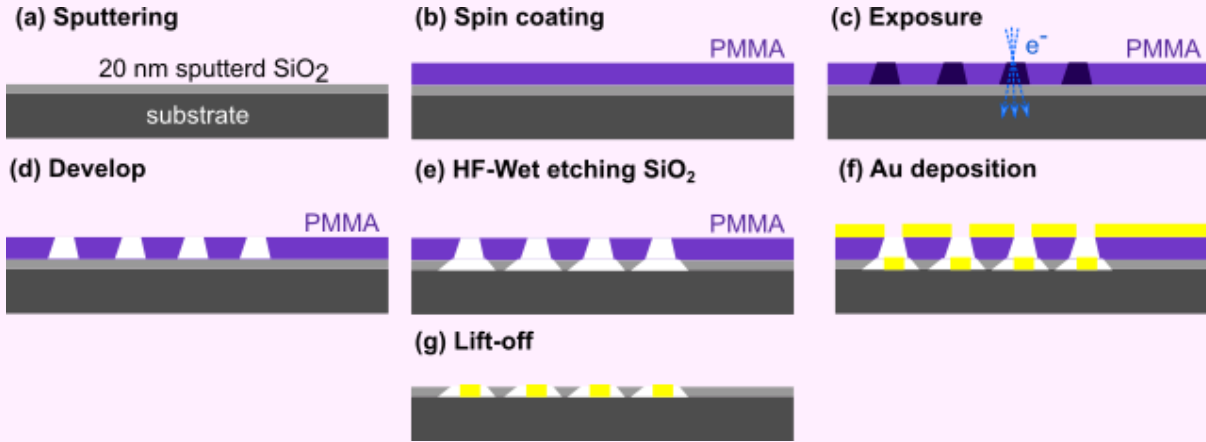
Part
3

Morphological evolution of InSb NFs

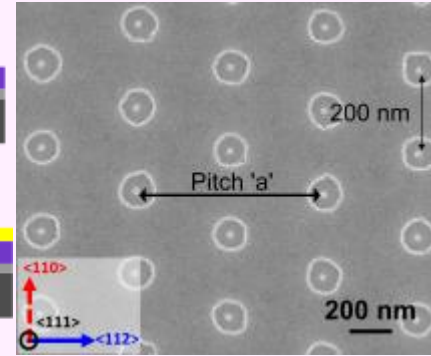


Morphological evolution of InSb NFs via Au-assisted SA growth

Lithographically patterned regular Au NP arrays on InP (111)B substrate



Top view SEM image

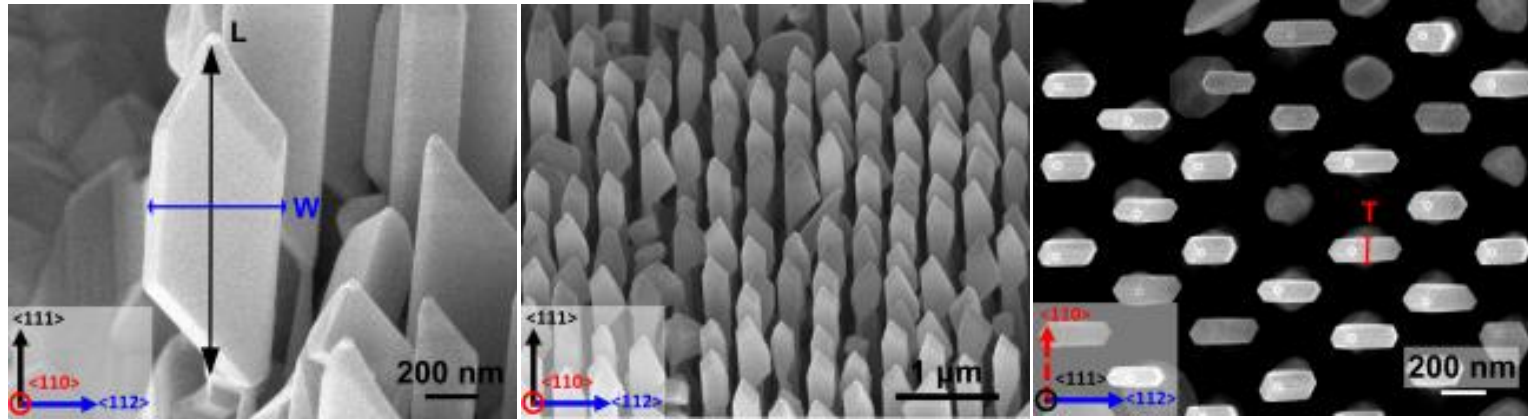


Au disc diameter = 30 ± 3 nm

- Pitch 'a': 500, 700, 900, 1100 and 1500 nm. Density: 3.6 to $12.3 \mu\text{m}^{-2}$.
- SiO_2 mask on InP(111)B to suppress the parasitic growth on the substrate surface.
- 60' InP NW growth 0.6/1.2 T_{InP} of $(405 \pm 5)^\circ\text{C}$

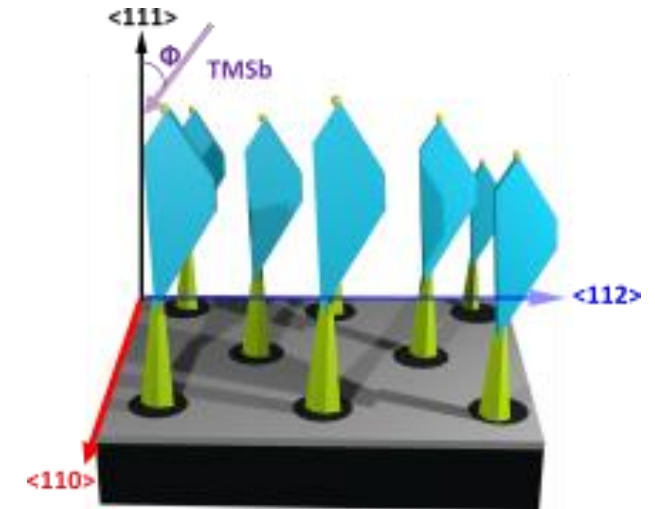


InSb NFs

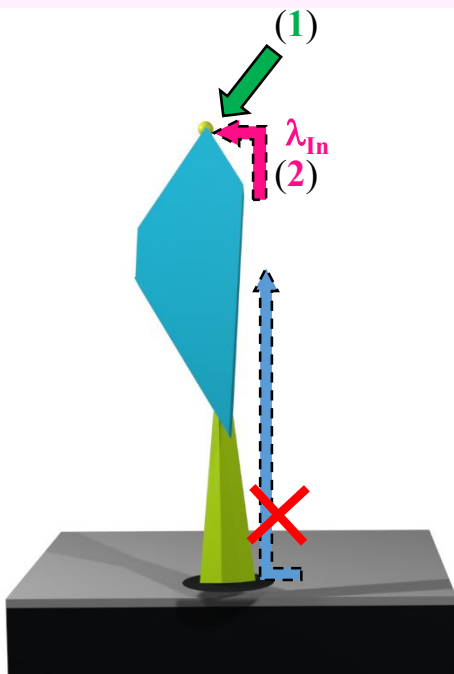
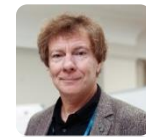


InP NW stem + 60' InSb 0.6/1.2 $\Delta T = -40^\circ\text{C}$

Model describing InSb NF growth and morphology as a function of time and pitch of the NW/NF array.



VLS axial growth



- Non-linear length evolution, considering the In-limited VLS axial growth rate containing two contributions: (1) the direct impingement and (2) In adatom diffusion on the NF sidewalls.

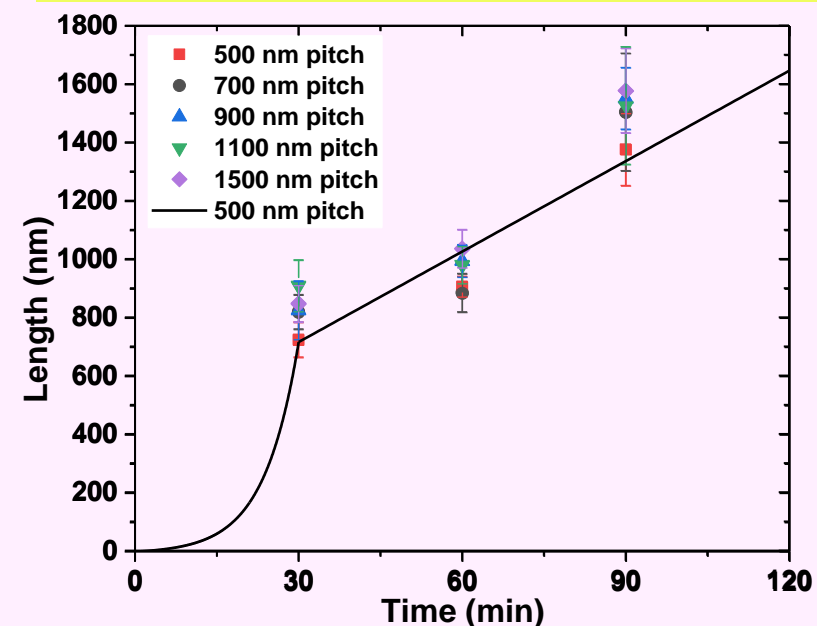
- Surface diffusion of In adatoms from the substrate → neglected as InP NW is $\sim 1.2 \mu\text{m}$ long.

- (1) is constant; In adatom diffusion from both InP and InSb sidewalls.
- When $L > \lambda_{\text{In}}$ (effective In diffusion length) contribution from sidewall diffusion decreases.
- Axial growth rates ↓ for smaller pitches due to shadowing or competition between the neighboring NFs for the material flux.
- For larger pitches ($a \geq 700 \text{ nm}$) the NF lengths are almost independent of the pitch, indicating no competition above this threshold.

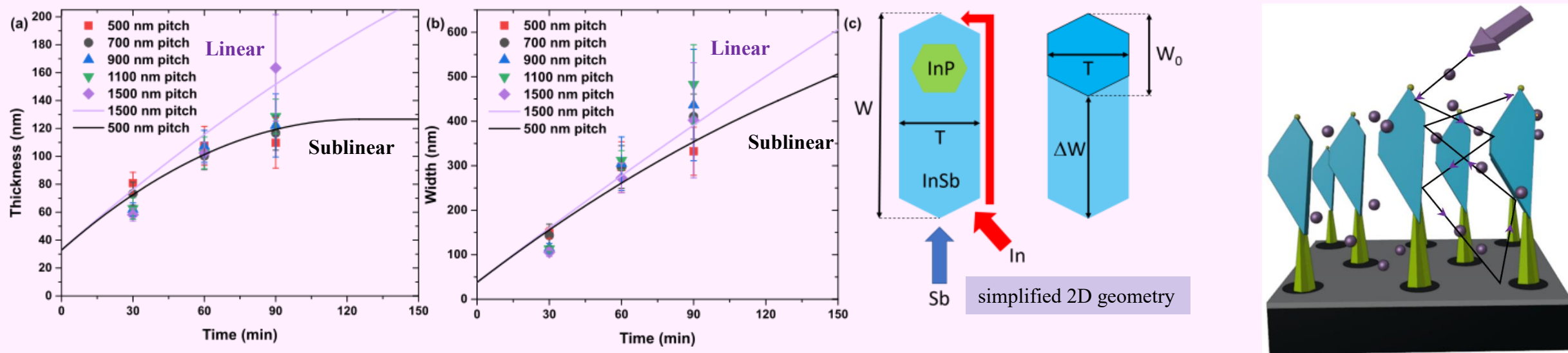
$$L = \frac{B}{A}(e^{At} - 1), L \leq \lambda_{\text{In}}; L = \lambda_{\text{In}} + (C\lambda_{\text{In}} + B)(t - t_0), L > \lambda_{\text{In}}$$

t_0 is the moment in time at which the NF length reaches λ_{In} . Fitting is done for $\lambda_{\text{In}} = 724 \text{ nm}$ at $a = 500 \text{ nm}$ with $A = 0.158 \text{ min}^{-1}$, $B = 1 \text{ nm/min}$, and $C = 0.013 \text{ min}^{-1}$

InSb NF L vs growth time for different pitches



VS radial growth

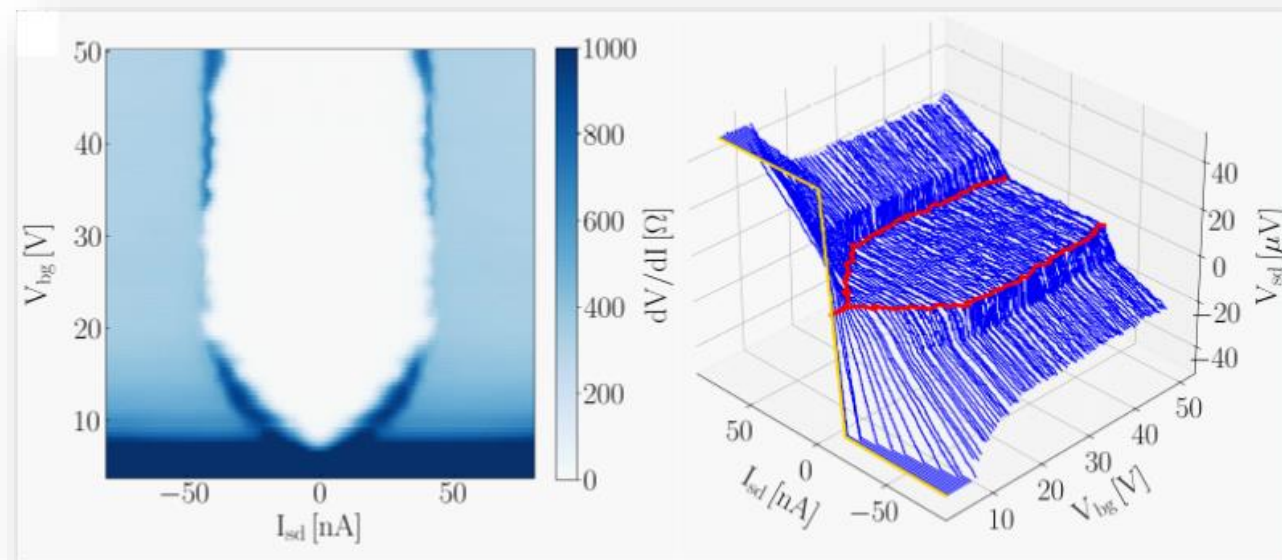


- VS radial growth rate of the InSb NFs, which controls the NF width and thickness, is 10 times lower than the VLS axial growth rate.
- Width and Thickness model takes into account direct, re-emitted fluxes of Sb, and the shadowing effect.
- Additional NF width is due to direct impingement of Sb flux on only 2 of the facets.
- In adatoms can reach the back side of the NF sidewall, while Sb atoms can impinge onto the back side only from re-emitted flux (non-directional).
- NF thickness \uparrow only due to re-emitted flux, which can be almost fully shadowed by \downarrow the pitch.

Thickness and width can be decoupled when re-emitted flux is completely suppressed!

Part 4

Electronic properties of InSb nanoflag based devices



Transport measurements- Field effect

Hall-bar device

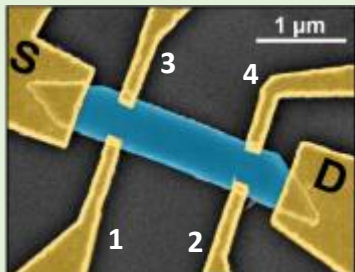
10 nm Ti/190 nm Au contacts

Substrate: Si/SiO₂

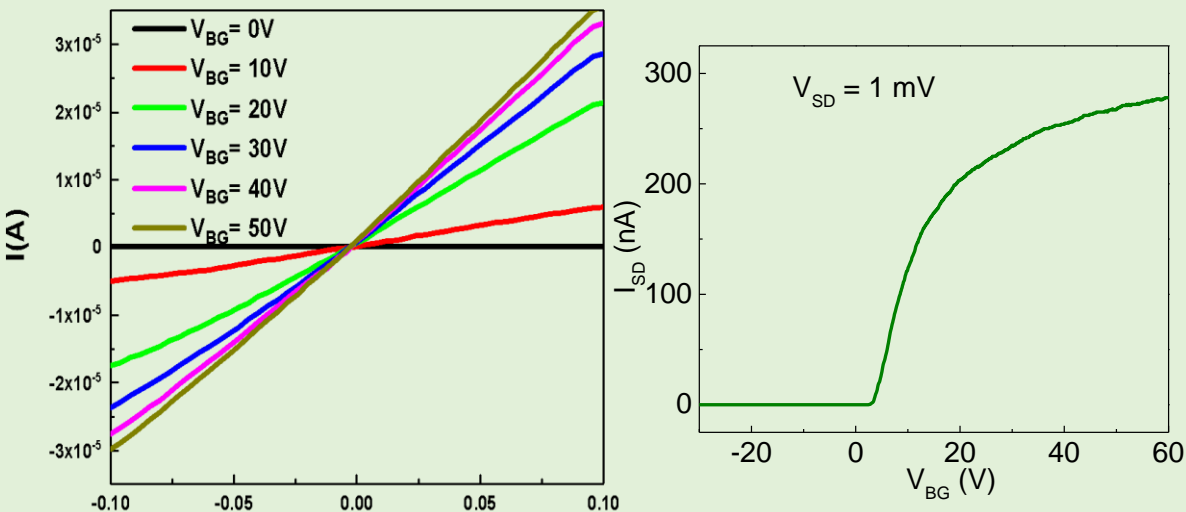
Channel width (width b/w contacts 1-3 & 2-4)=325 nm

Channel length (1-2 and 3-4)=1.5 μm

The NF thickness is ~100 nm.



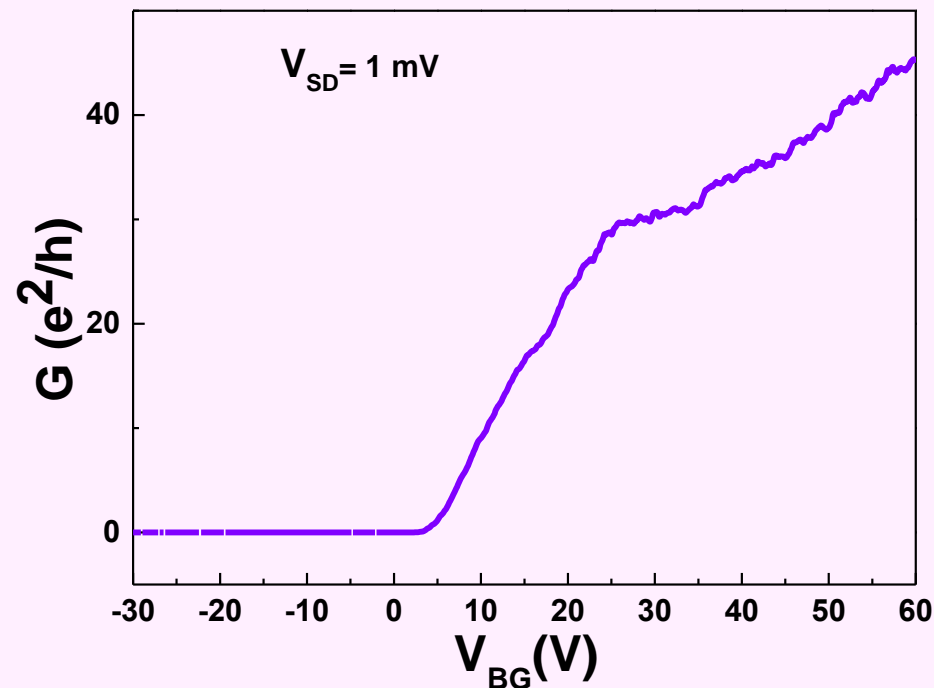
I_{SD}-V_{SD} curves of the S-D channel at 4.2 K as a function of V_{BG}



$R_{SD}(RT, V_{BG}=0 \text{ V}) = 11 \text{ K}\Omega$
 $R_{SD}(4.2\text{K}, V_{BG}=50 \text{ V}) = 2.5 \text{ K}\Omega$

- Presence of good ohmic contacts between InSb NF and the metal contacts.
- Absence of Schottky barrier.
- Variation of injected current vs BG voltage: **n-type** characteristic of InSb NFs under BG modulation. No ambipolar behavior.

Four-probe configuration at 4.2K



$$\mu_{FE} = 28000 \text{ cm}^2/\text{V}\cdot\text{s}$$

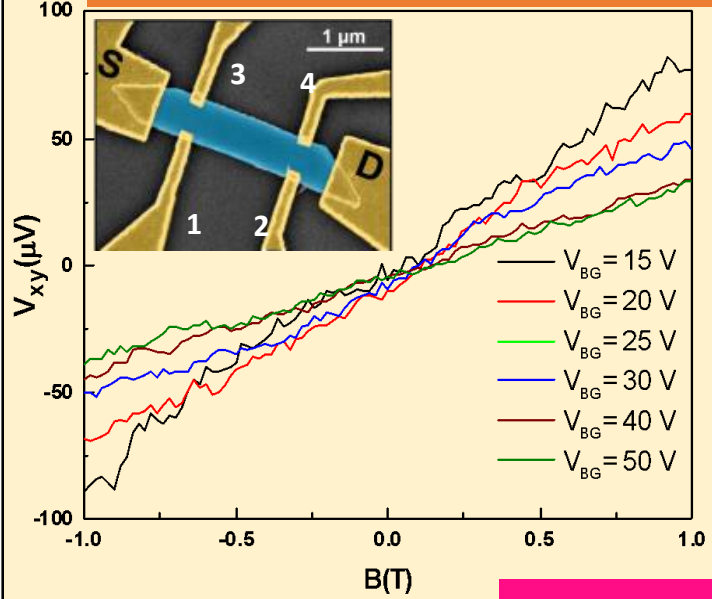
- The four-probe field effect mobility is then obtained using the formula:

$$\mu_{4pFE} = \frac{L}{WC_{ox}} \left(\frac{dG}{dV_{BG}} \right)$$

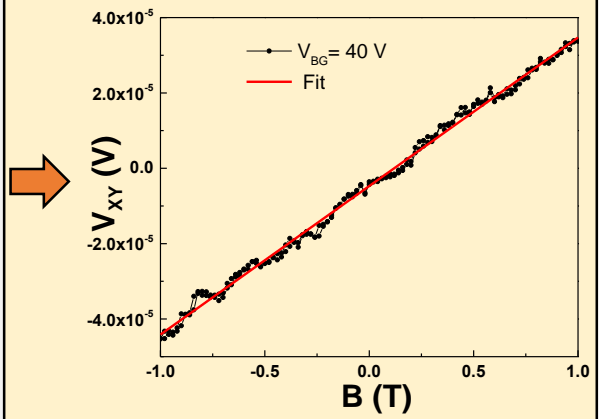
with $L/W = 4.6$ and $C_{ox} = 10 \text{ nF/cm}^2$

Transport measurements- Hall measurements

Low-field Hall measurement @ 4.2K

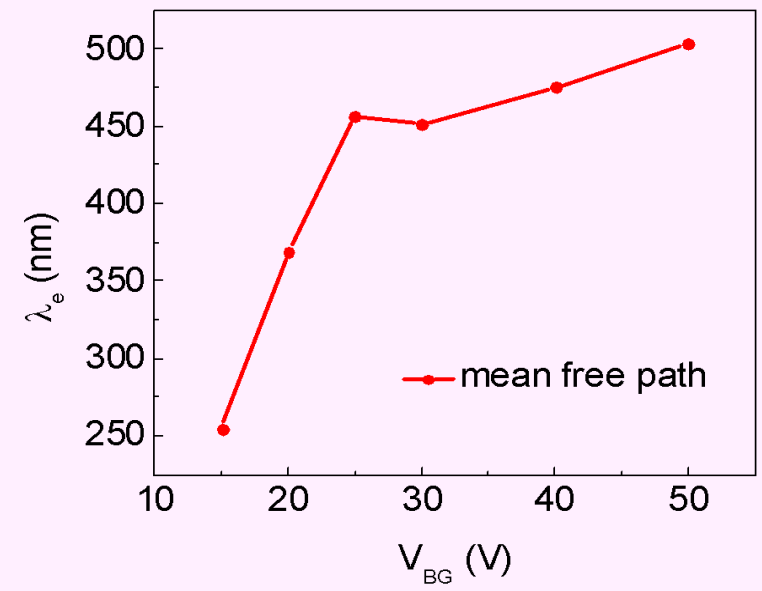
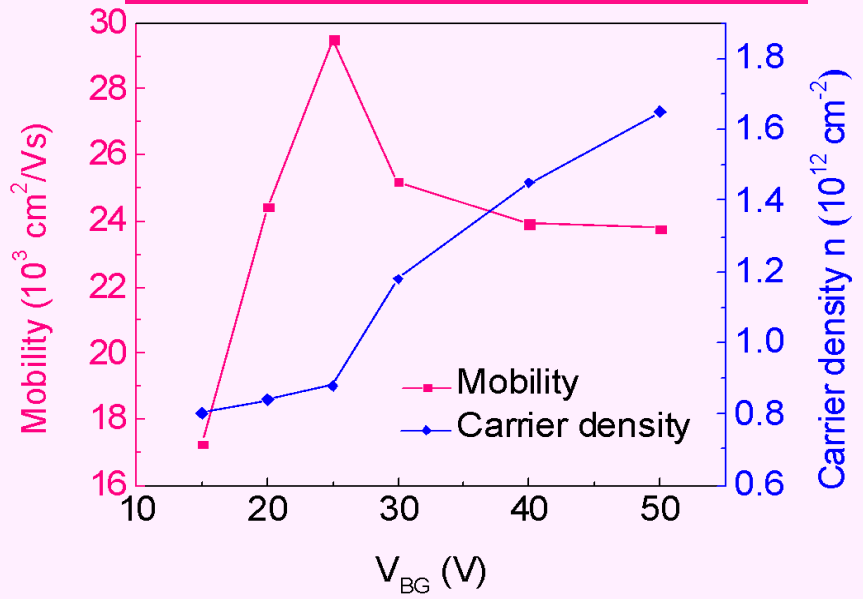


- Performed using a constant AC bias of 100 nA at 4.2K. Minimum V_{BG} of 15V is required at which channel is well open.
- Forward and backward sweep of the $B(T)$, to demonstrate reproducibility of measurement, plus the fit to the experimental data, from which the carrier concentration is obtained.
- Hall mobility μ_H , carrier concentration n and mean free path lengths for each back gate voltage is calculated using the formulas:

$$\mu_H = \frac{L}{W \langle V_{xx} \rangle} \left(\frac{V_{xy}}{B} \right) ; n = \frac{1}{e} \left(\frac{B}{V_{xy}} \right) ; \lambda_e = (\hbar \mu / e) (2\pi n)^{1/2}$$


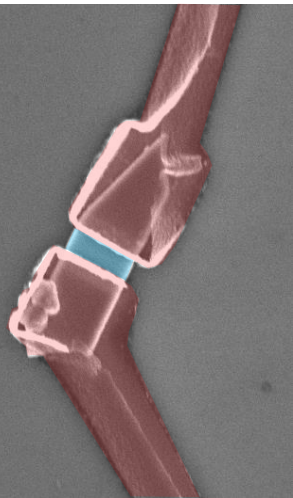
Electron Hall mobility = 29500 cm²/Vs

Mean free path l_e up to 500 nm



Nb/Ti-InSb nanoflag based JJs

2 μm

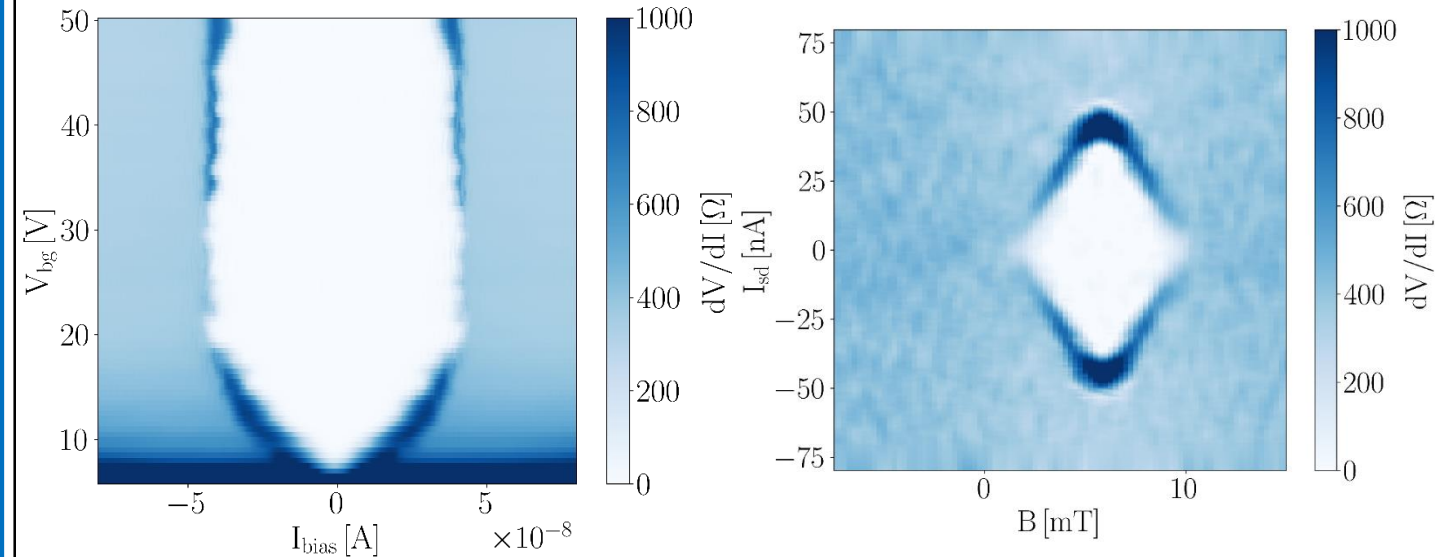
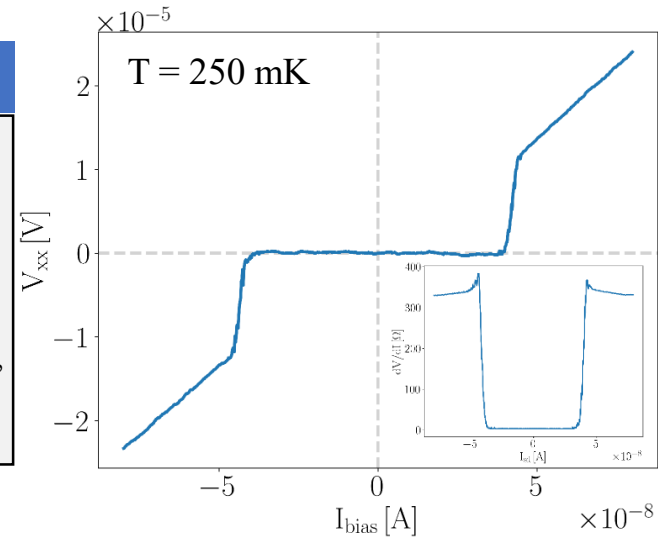


10 nm Ti/150 nm Nb contacts
Substrate: Si/SiO₂
Channel length $L=200$ nm
Channel width $W=700$ nm
The NF thickness $d \sim 100$ nm.
Ballistic regime!
Mean free path $\lambda_e >$ length L of the junction,
 $\lambda_e > L$.

Josephson Junction Device

V-I characteristic at $V_{BG}=30\text{V}$

- Dissipationless transport.
- Proximity-induced superconductivity in the InSb NF.
- Bias current exceeds the critical value of 50 nA, superconductive \rightarrow normal state transition, with $\sim 330 \Omega$ resistance.



Color scale plots

dV/dI vs I_{SD} and V_{BG}

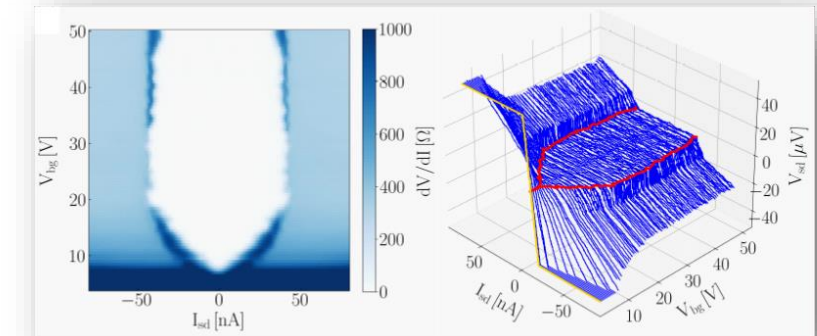
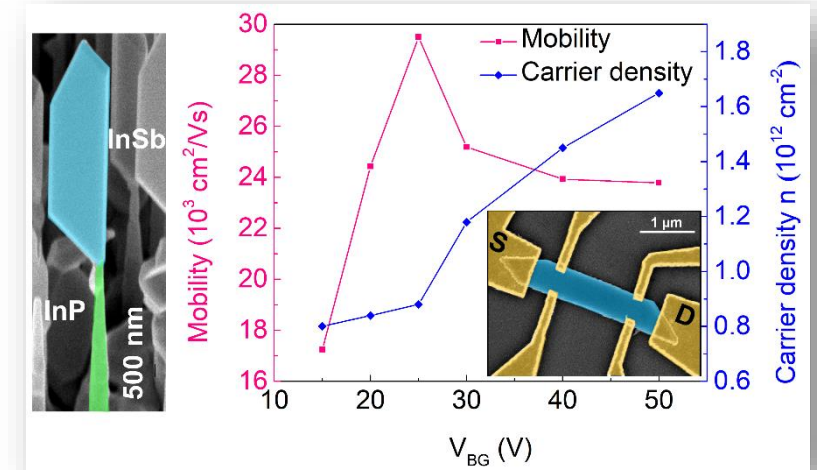
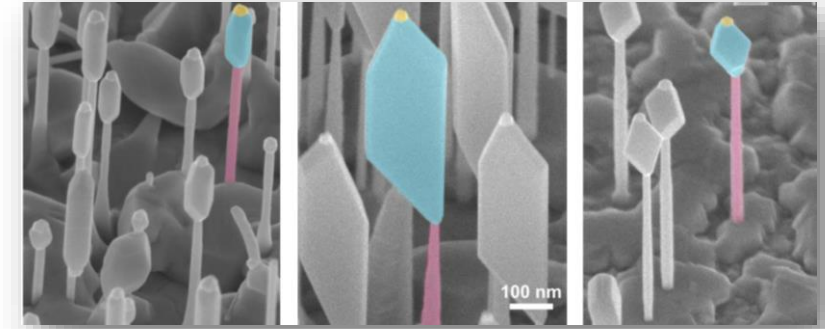
- Central white region represents the zero-resistance supercurrent branch.
- V_{bg} from 20 to 50 V, supercurrent ~ 50 nA.
- $V_{bg} < 20$ V, supercurrent decreases, until it disappears for 5V.
- Gate tunable supercurrent.

dV/dI vs I_{SD} and B

- Superconducting quantum interference was observed in the dependence of the supercurrent on a B applied perpendicular to sample plane.
- Supercurrent maxima is obtained at $B_0=6$ mT. Offset due to residual magnetisation in the cryostat.
- $|B-B_0| > 5.2$ mT, supercurrent suppressed.
- Modulation of I_c by quantum interference is one of the hall marks of Josephson effect.

Conclusions

- Finding the parameters that affect axial and radial growth is important for controlling and tuning the nanostructure morphology.
- More robust NW stem for longer growth time and sustenance of orientation.
- A simplified 2D growth model was presented which allowed for semi-quantitative description of the NF morphology as a function of the growth time and pitch. W and T decoupling.
- Electron Hall mobility of about $29500 \text{ cm}^2/\text{V}\cdot\text{s}$ reported for free-standing InSb NF. Mean free path upto 500 nm.
- InSb NFs: versatile and convenient 2D platform for advanced quantum technologies.



Acknowledgments

Growth Activity



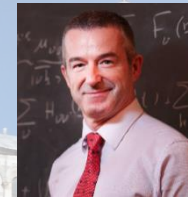
Valentina Zannier



Daniele Ercolani

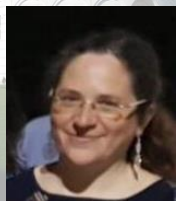


Lucia Sorba



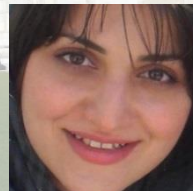
Fabio Beltram

TEM Characterization



Francesca Rossi

Transport Measurements



Sedighe Salimian



Stefan Heun

Theoretical Modeling



Vladimir Dubrovskii

Thank you for your attention!

